Electronic Supplementary Information (ESI†)

Real time detection of the nerve agent simulant diethylchlorophosphate by non fluorophoric small molecules generating cyclization induced fluorogenic response

Syed Samim Ali,[a] Ankita Gangopadhyay,[a] Ajoy Kumar Pramanik,[a] Sandip Kumar Samanta,[a] Uday Narayan Guria,[a] Srimanta Manna [a] and Ajit Kumar Mahapatra*[a]

[a]Department of Chemistry, Indian Institute of Engineering Science and Technology, Shibpur, Howrah – 711103, India.

*Corresponding author: Tel.: +91 33 2668 4561; fax: +91 33 26684564;
E-mail: mahapatra574@gmail.com

Chemical structure of nerve agents and Simulants:

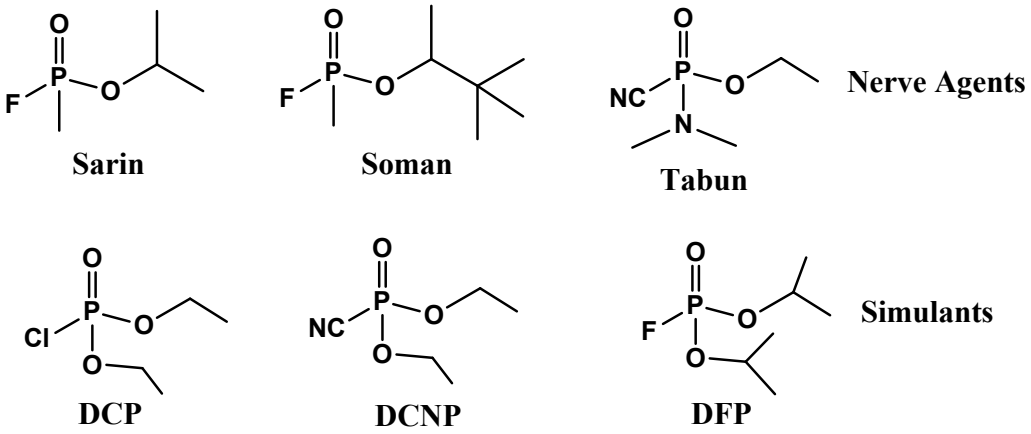

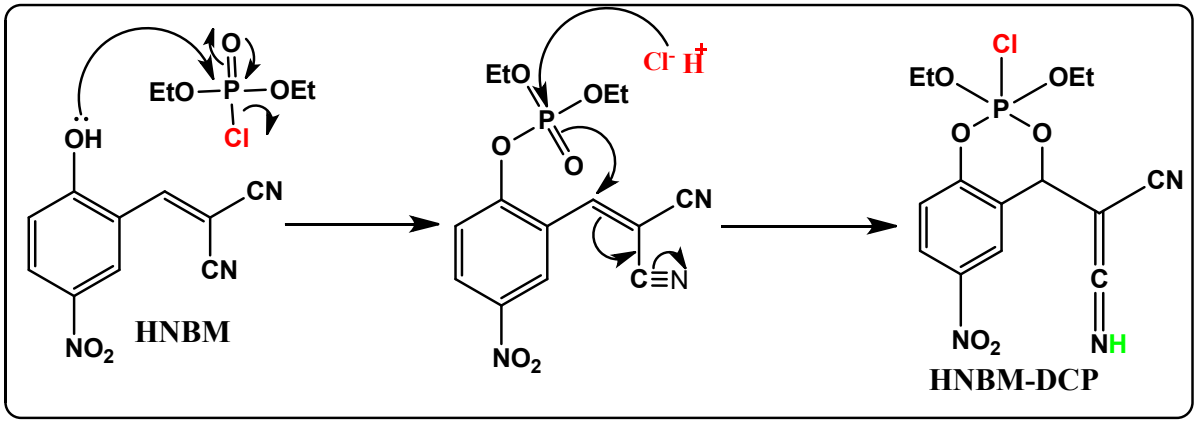

Fig. S1 Plausible Mechanism of DCP binding

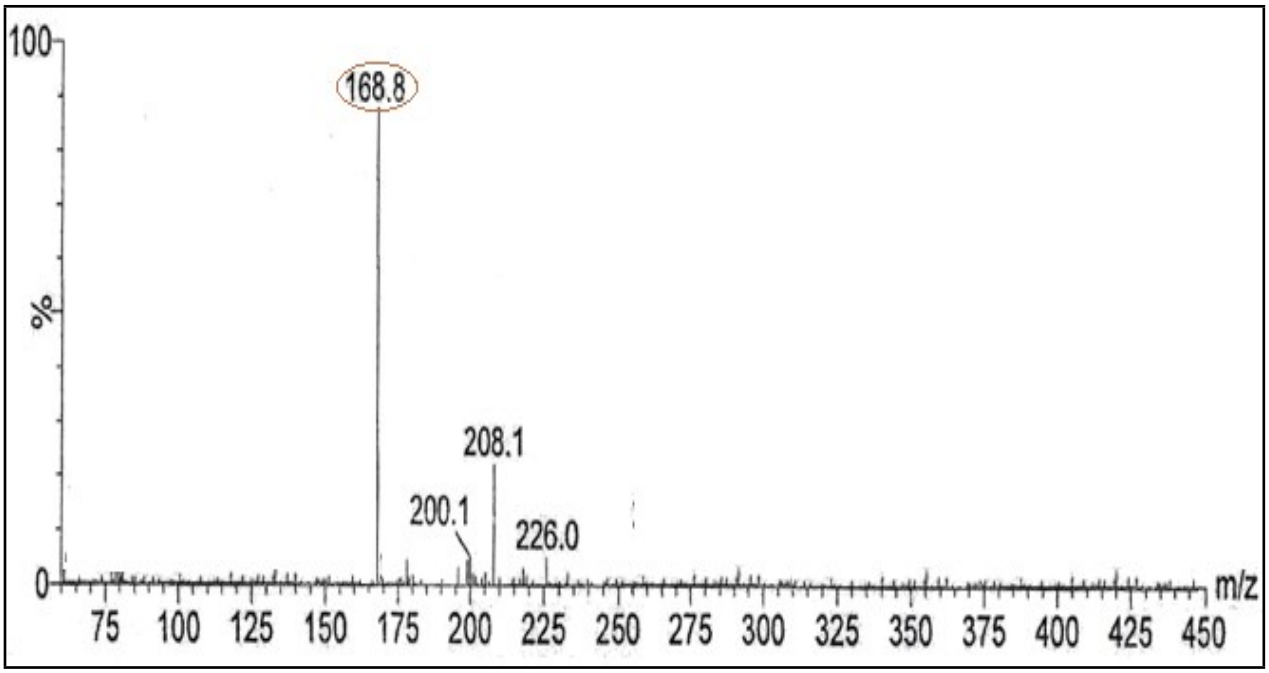

Fig. S2 LCMS of compound **2a**

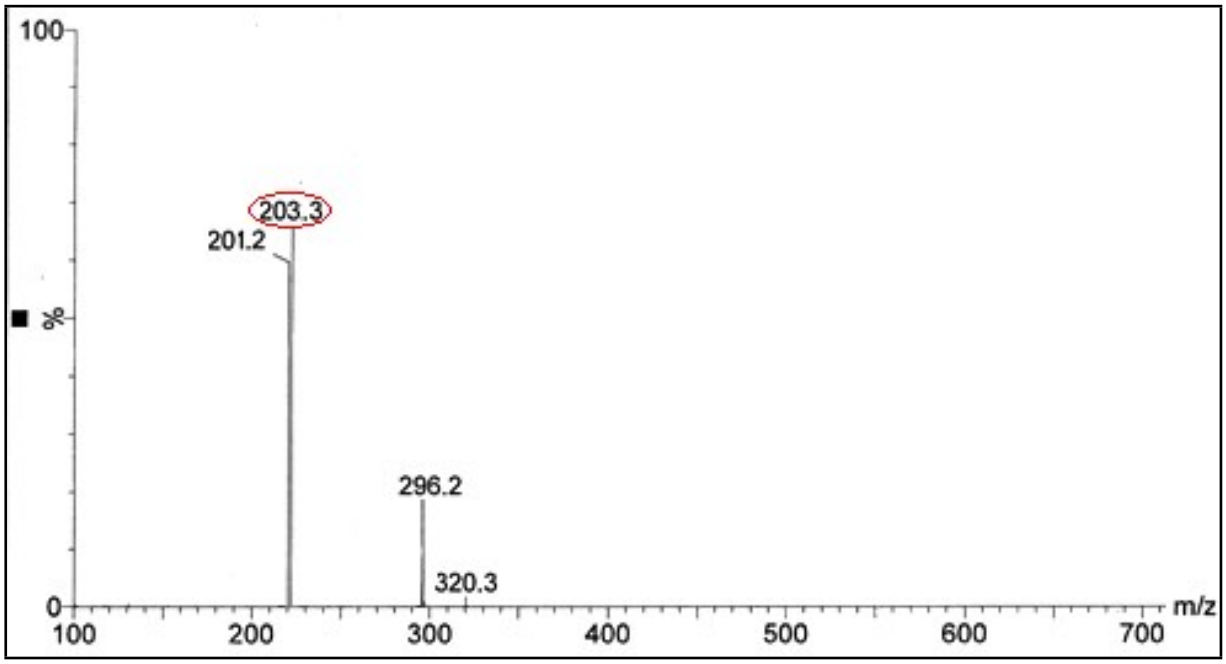

Fig. S3 LCMS of compound **2b**

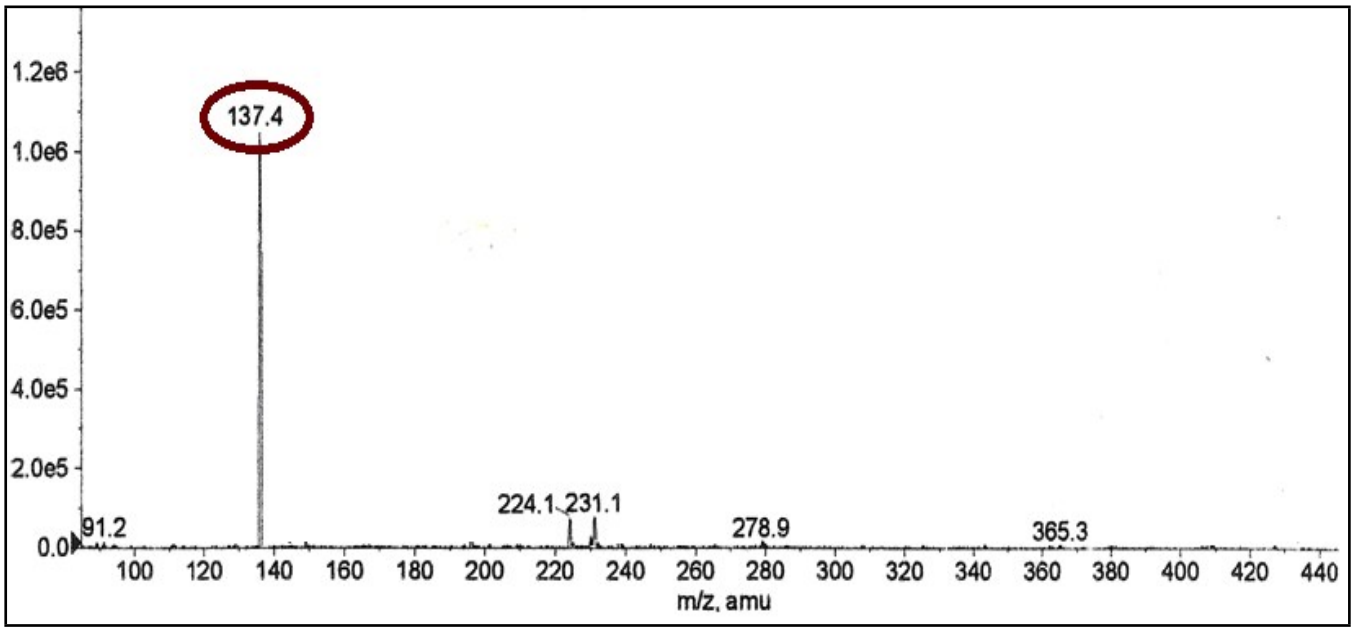

Fig. S4 LCMS of compound **2c**

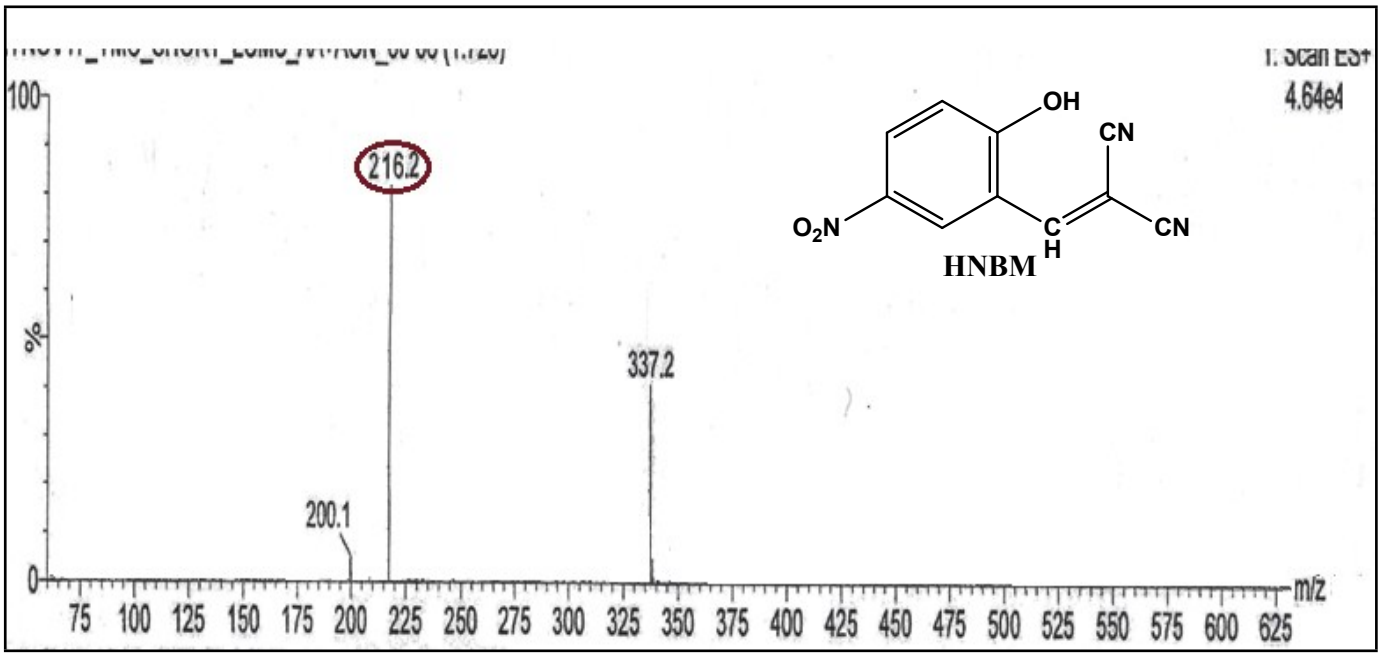

Fig. S5 LCMS of compound **HNBM**

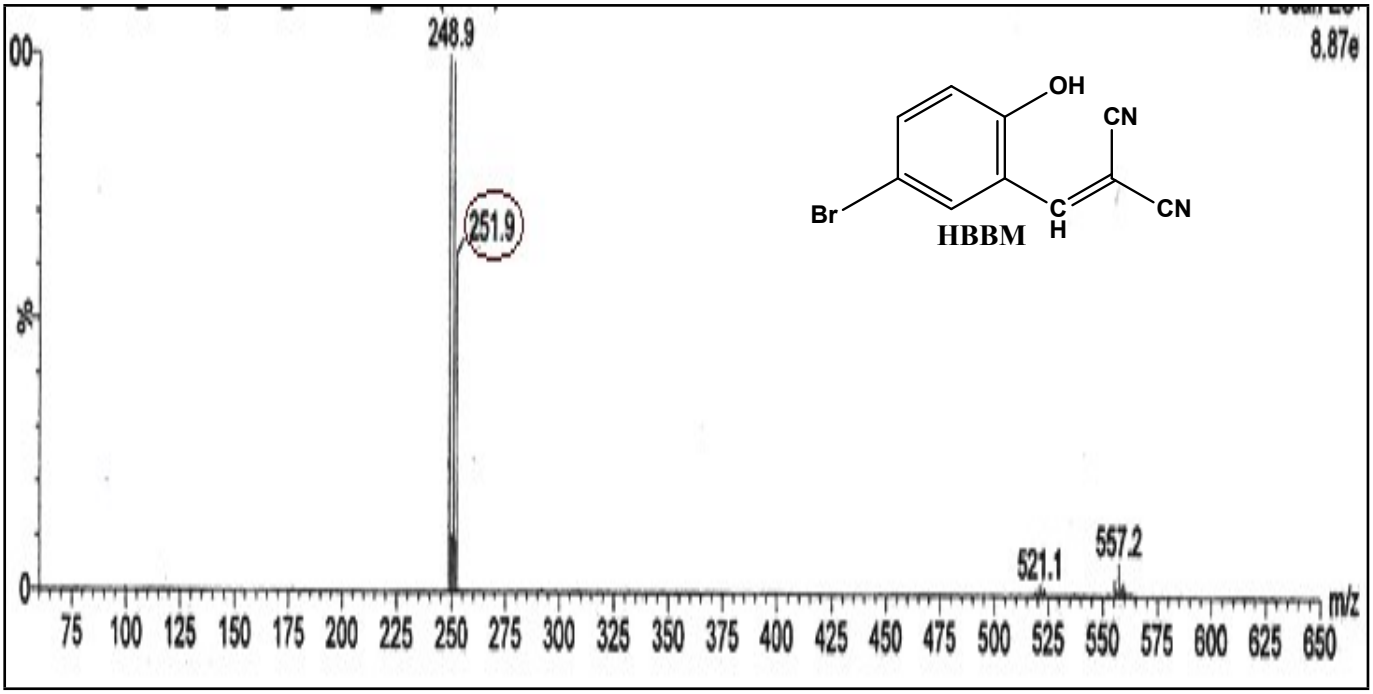

Fig. S6 LCMS of compound **HBBM**

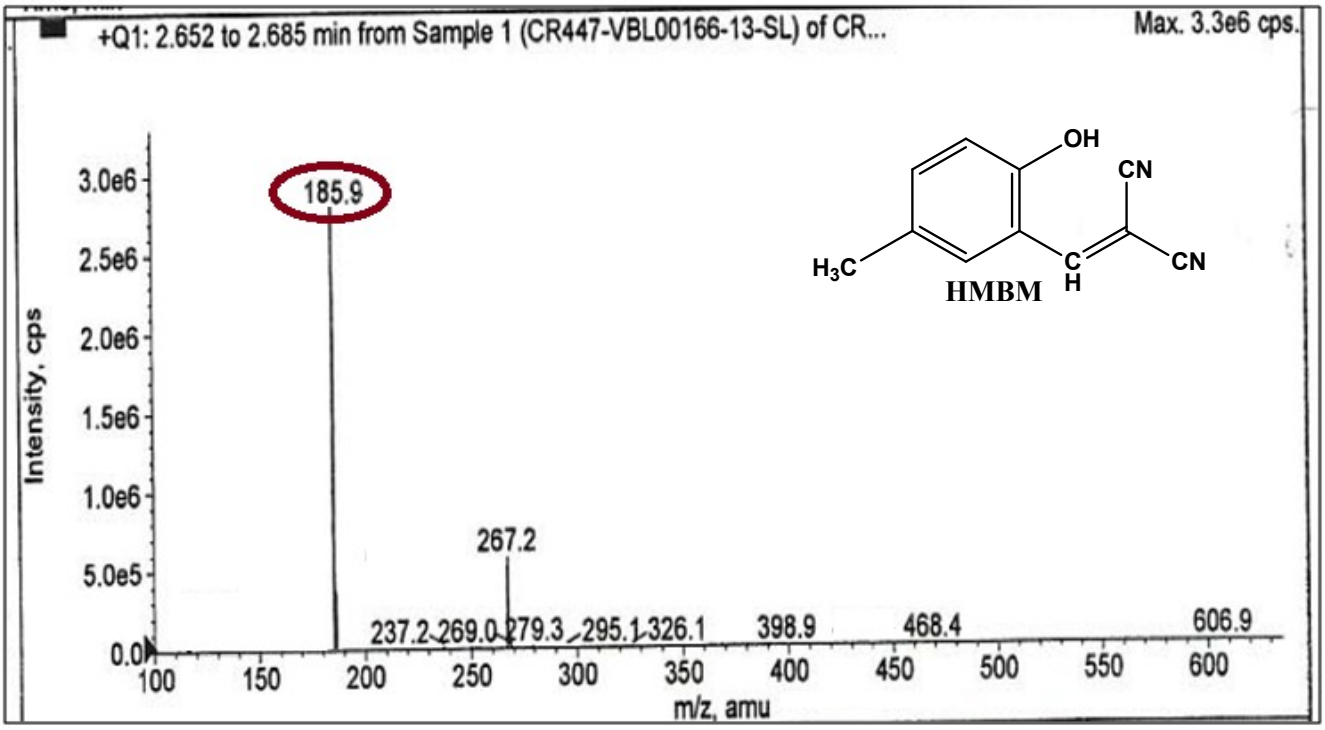

Fig. S7 LCMS of compound **HMBM**

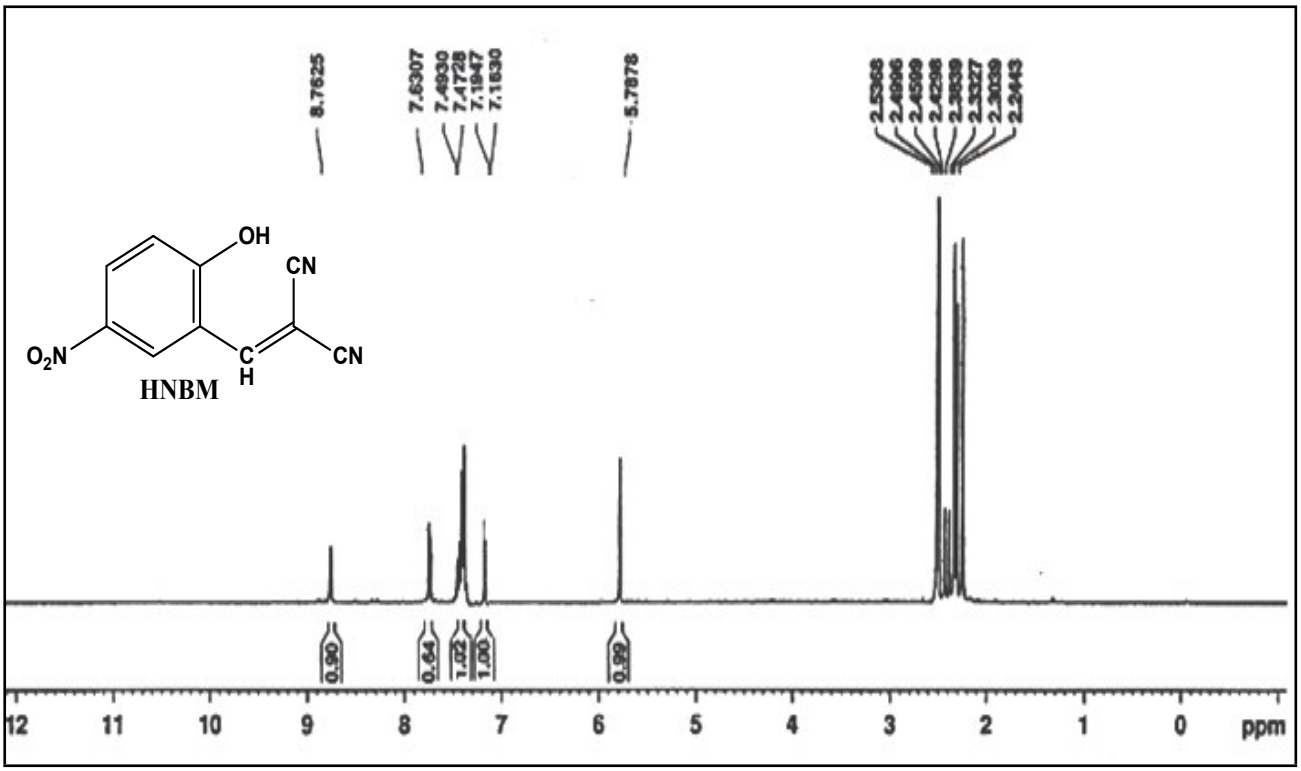

Fig. S8 ^{1}H NMR of **HNBM** in (d6-DMSO).

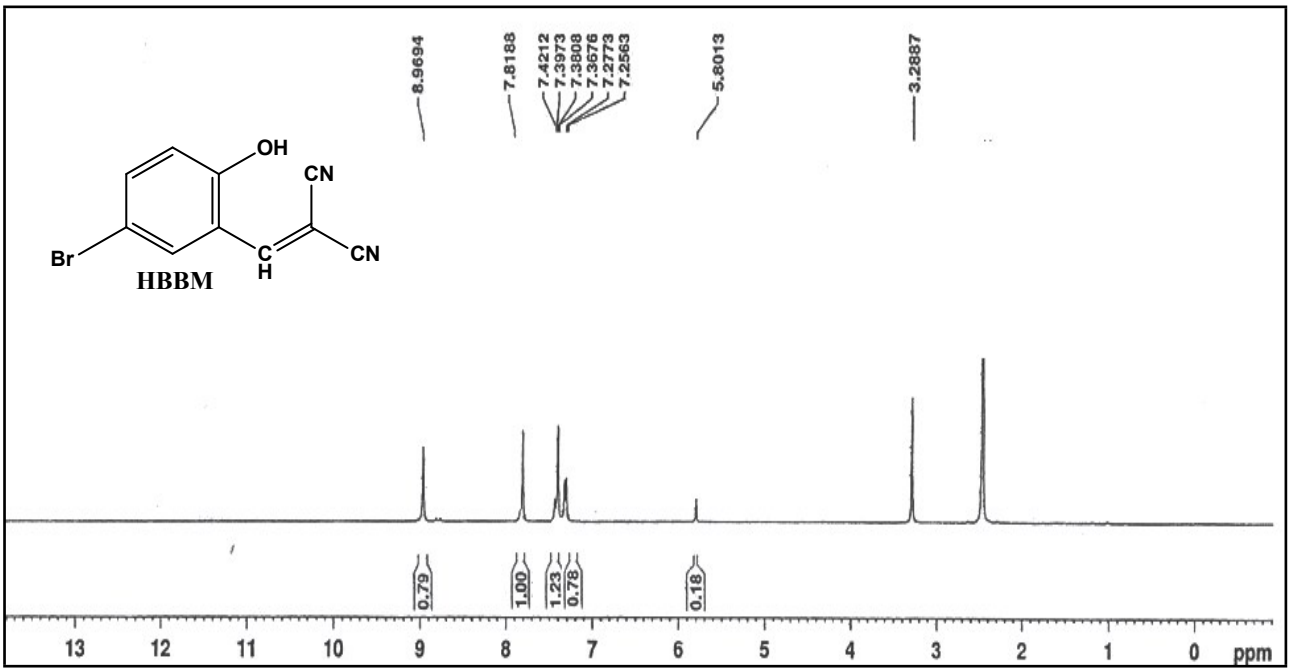

Fig. S9 ^{1}H NMR of **HBBM** in (d6-DMSO).

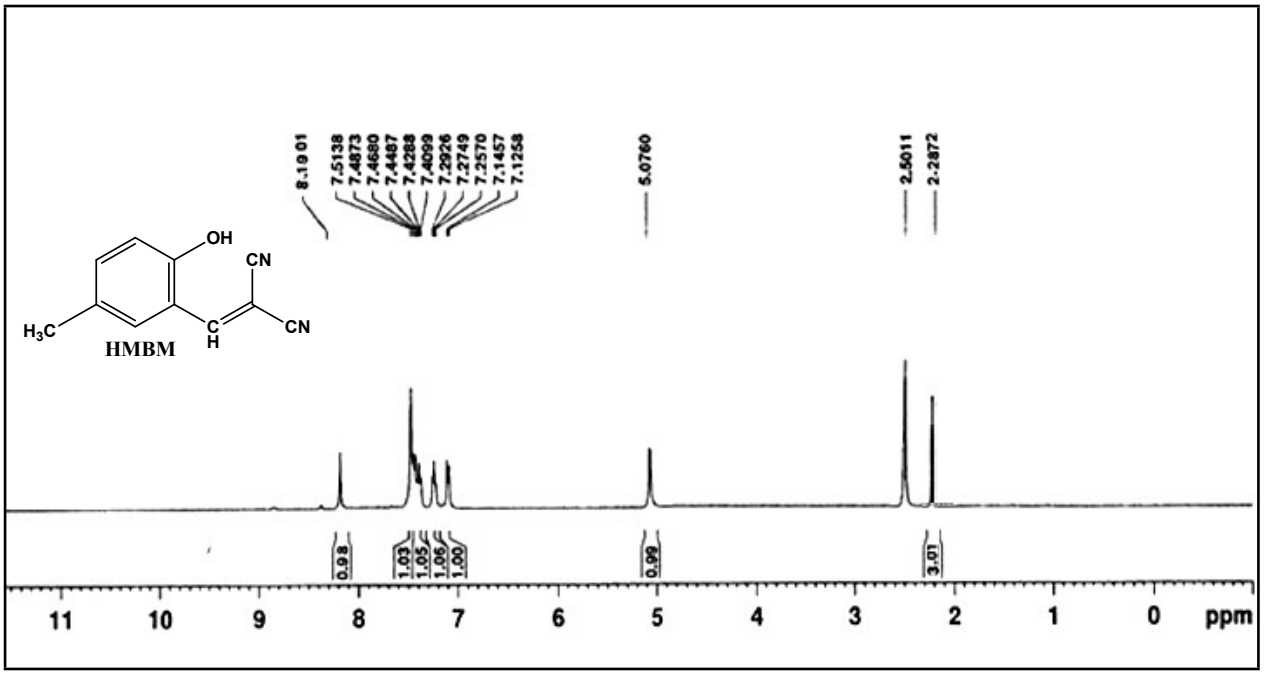

Fig. S10 1H NMR of **HMBM** in (d6-DMSO).

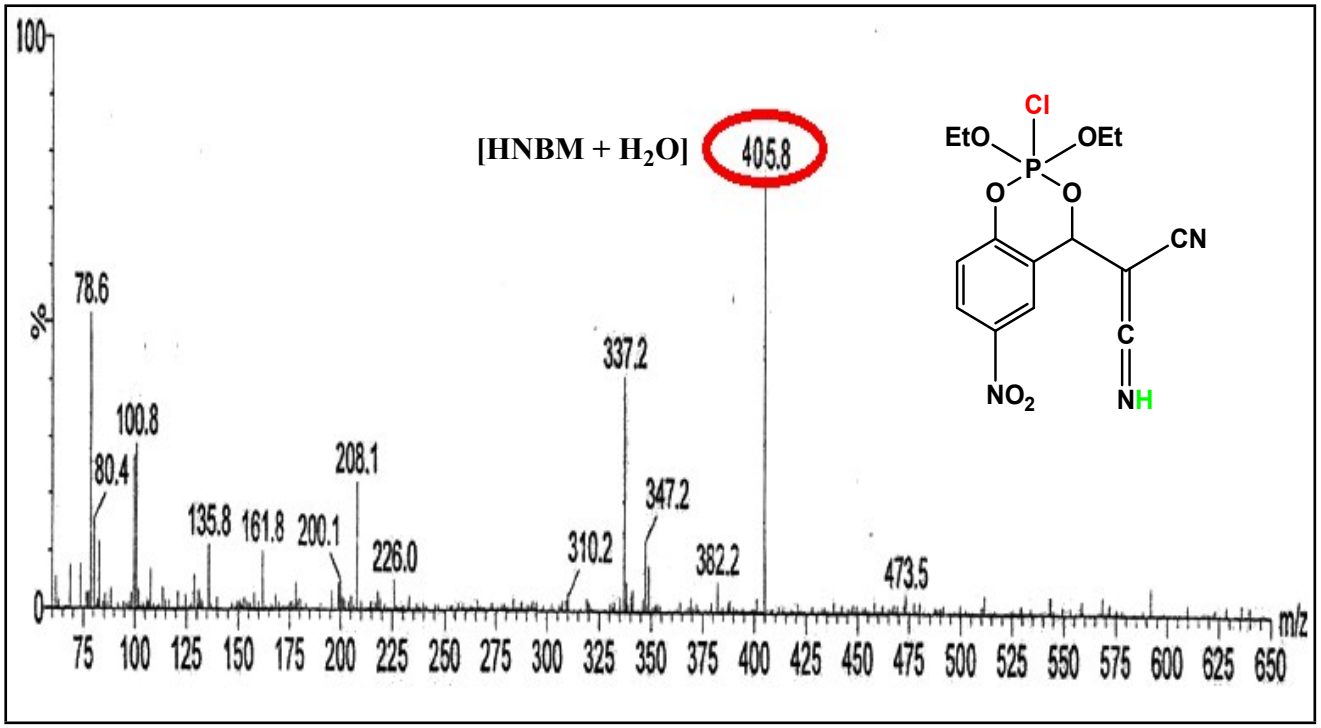

Fig. S11 LCMS spectra of **HNBM-DCP** Complex.

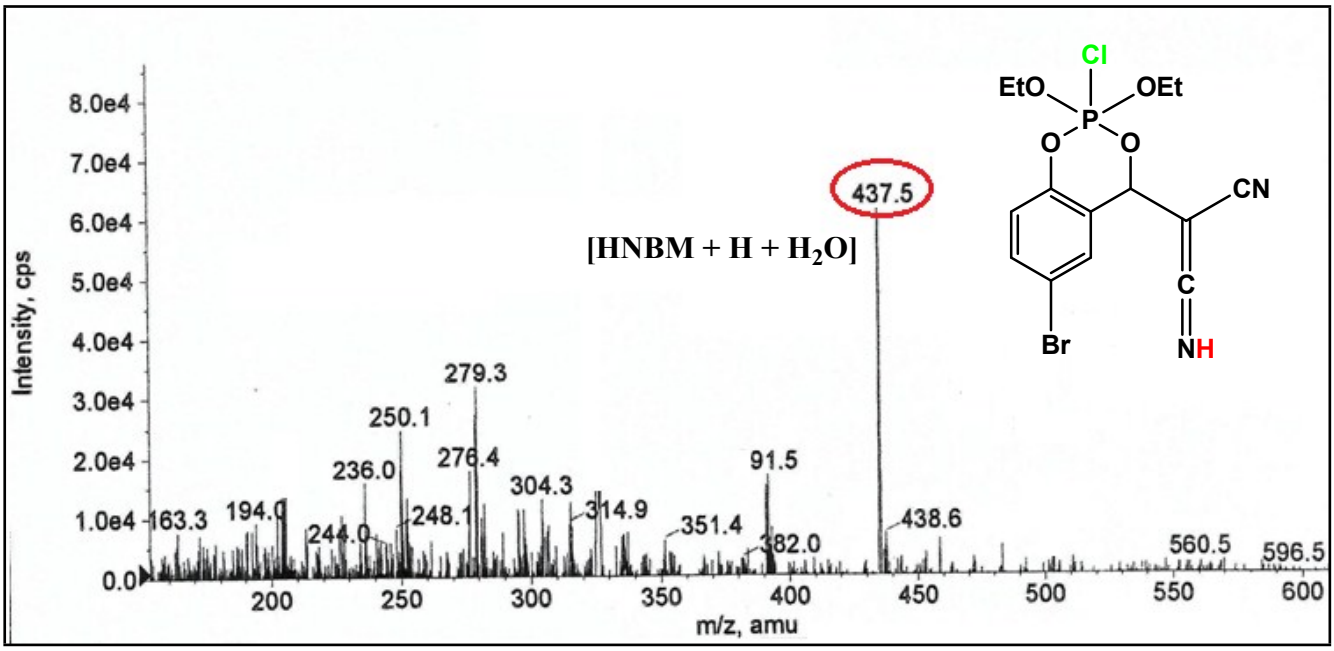

Fig. S12 LCMS spectra of **HBBM-DCP** Complex .

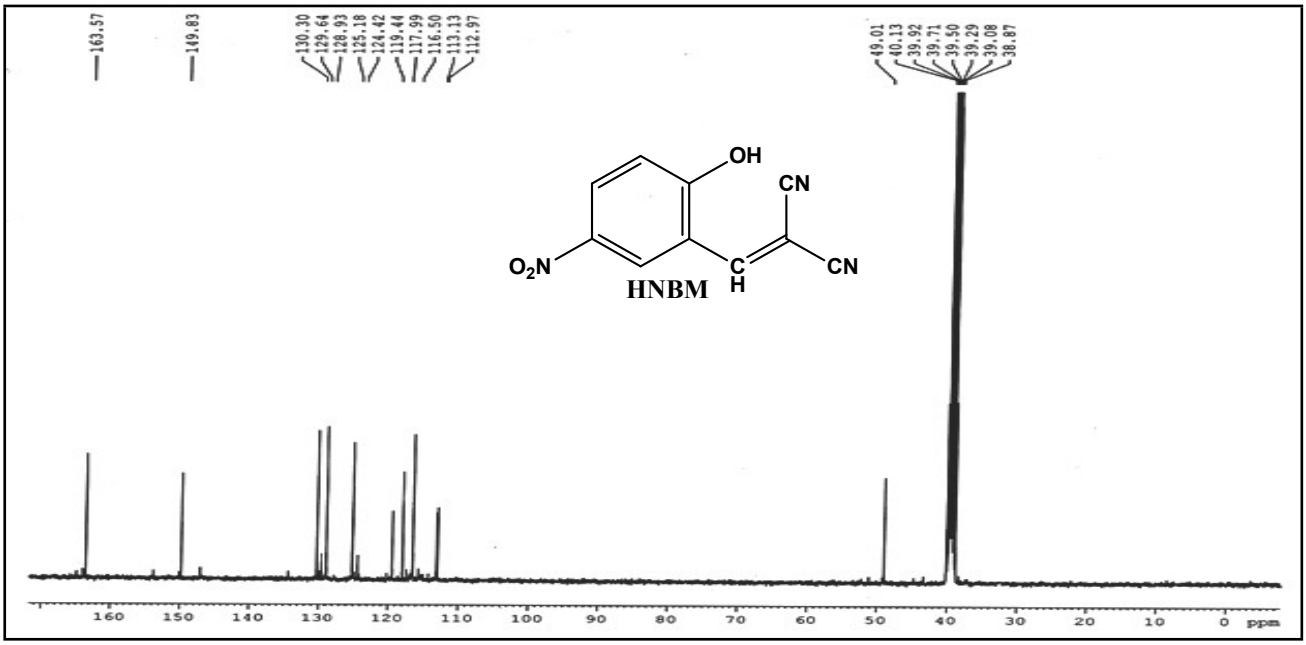

Fig. S13 C^{13} NMR spectra of **HNBM**.

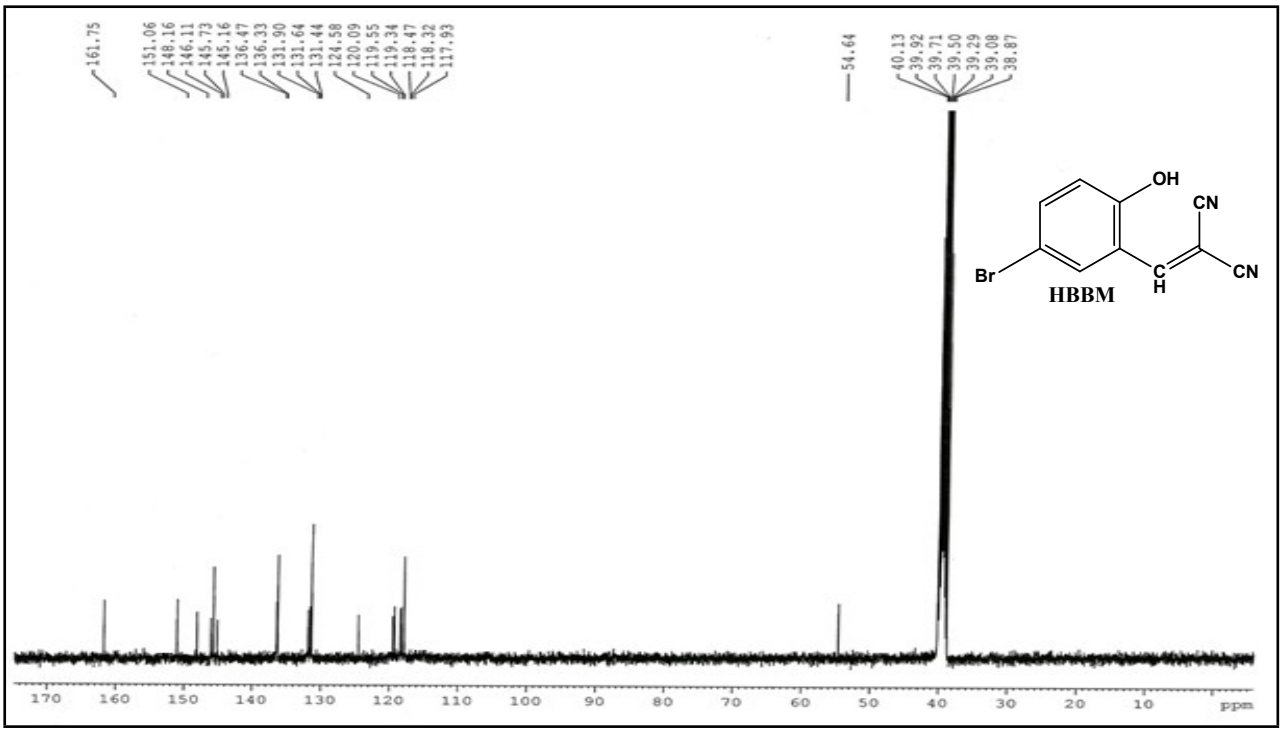

Fig. S14 C^{13} NMR spectra of **HBBM**.

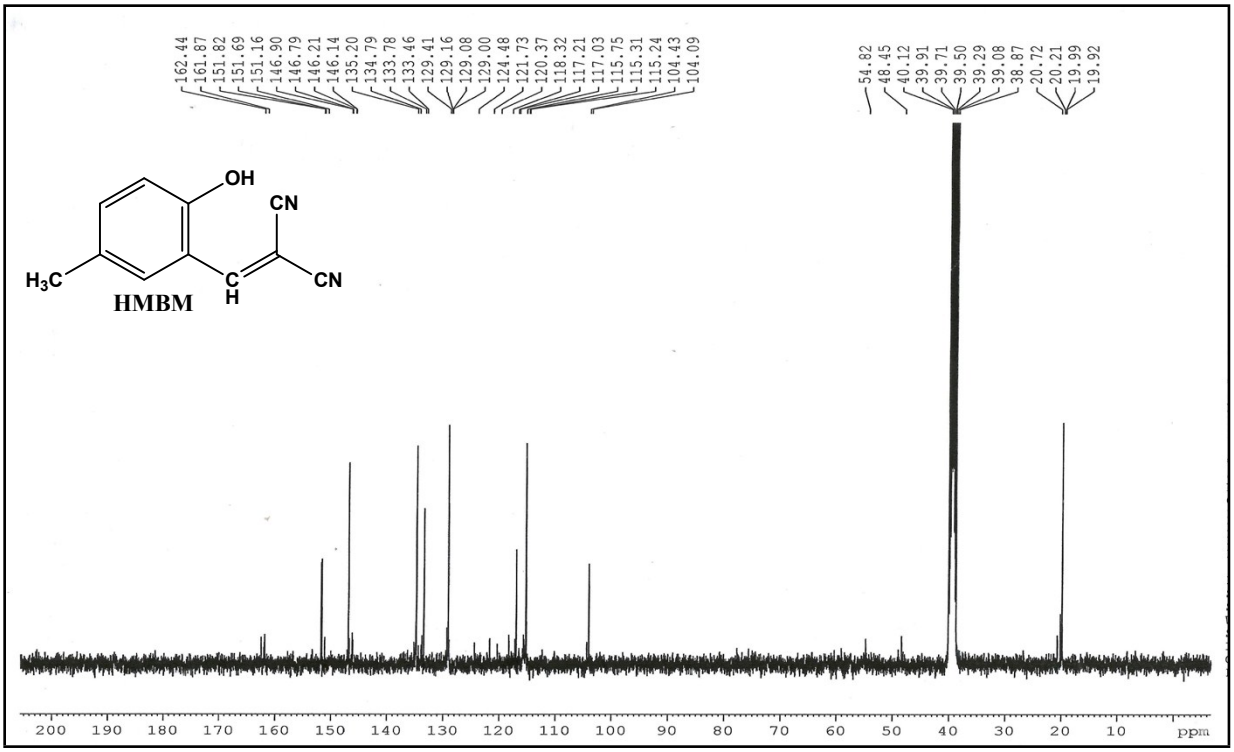

Fig. S15 C^{13} NMR spectra of **HMBM**.

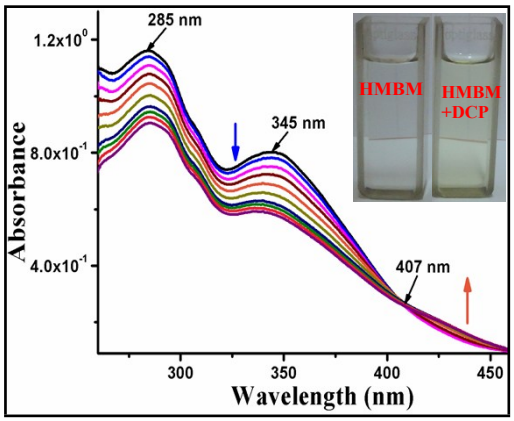

Fig. S16 Absorption spectra of **HMBM** (2 μM) in acetonitrile−water (7:3) upon addition of increasing amount of DCP (40 μM).

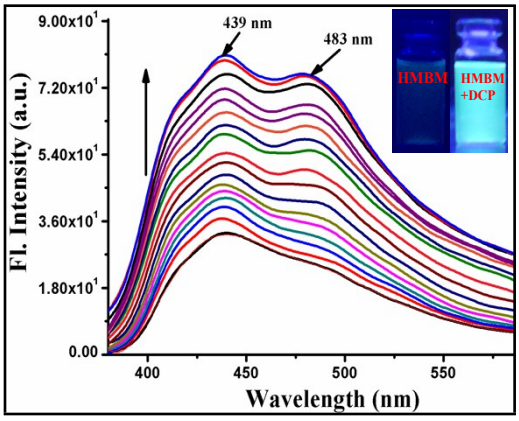

Fig. S17 Fluorescence spectra of **HMBM** (2 μM) in acetonitrile−water (7:3) upon addition of increasing amount of DCP (40 μM), λ_{exc} =345 nm.

Calculation of Detection limit:

The detection limit (DL) of **NTBT** for DCP were determined from the following equation:

DL = K* Sb1/S

Where K = 2 or 3 (we take 3 in this case); Sb1 is the standard deviation of the blank solution; S is the slope of the calibration curve.

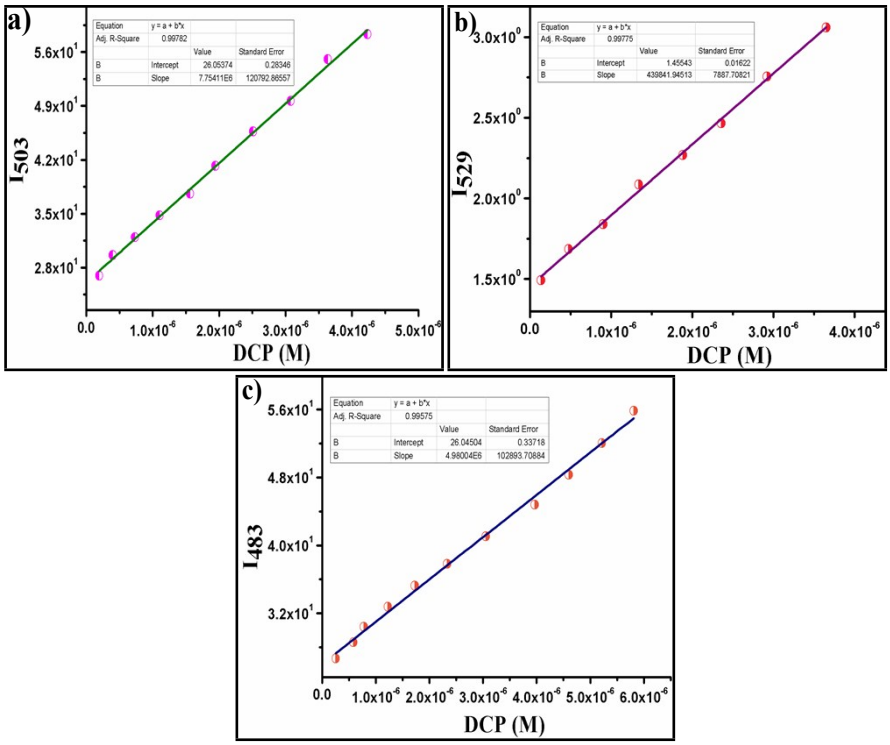

Fig. S18 (a) LOD calculated from fluorescence data for **HNBM** with DCP in CH_3CN at λex = 373 nm, λem = 503 nm. LOD is 0.10 μM (b) LOD calculated from fluorescence data for **HBBM** with DCP in CH_3CN at λex = 398 nm, λem = 529 nm. LOD is 0.11 μM (c) LOD calculated from fluorescence data for **HMBM** with DCP in CH_3CN at λex = 345 nm, λem = 483 nm. LOD is 0.20 μM.

Job's Plot:

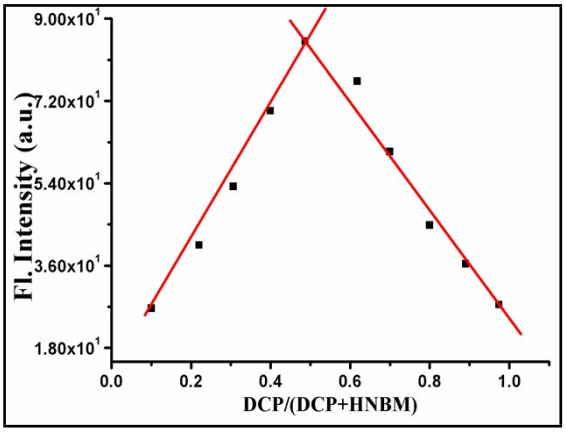

Fig. S19 Fluorescence Job's plot of **HNBM** with **DCP**.

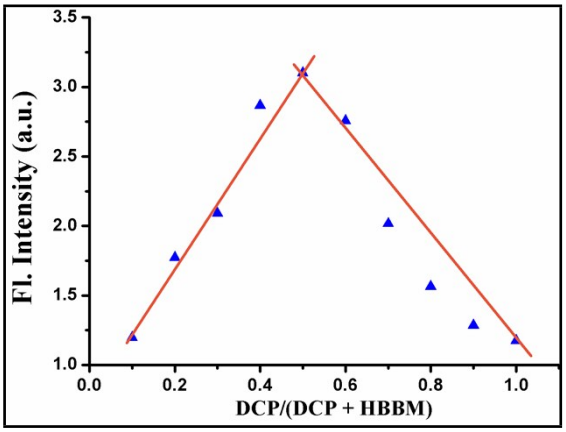

Fig. S20 Fluorescence Job's plot of **HBBM** with **DCP**.

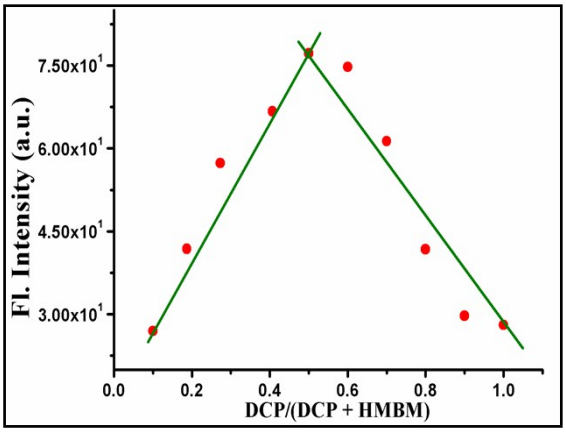

Fig. S21 Fluorescence Job's plot of **HMBM** with **DCP**.

Kinetic Study:

The rate of the cyclization was determined by fitting the fluorescence intensities of the samples to the Pseudo-First Order Equation (1):

$Ln(F_{max}-F_t)/F_{max}= -kt$…….(1)

Where F(t) and F(max) are the fluorescence intensities at the monitoring wavelengths at times t and the maxima values which are the last fluorescence intensities when the cyclization of **NTBT** reached the conversion of 100%. The k is the apparent rate constant.

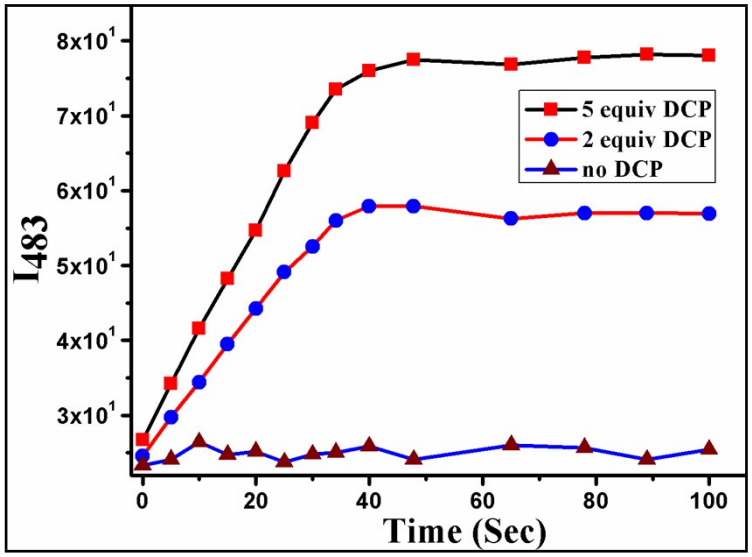

Fig. S22 Time-dependent fluorescence intensity of **HMBM** (2 μM) at 483 nm with incremental (0- 5 equiv) addition of DCP (40 μM) excitation at 345 nm.

Rate Constant:

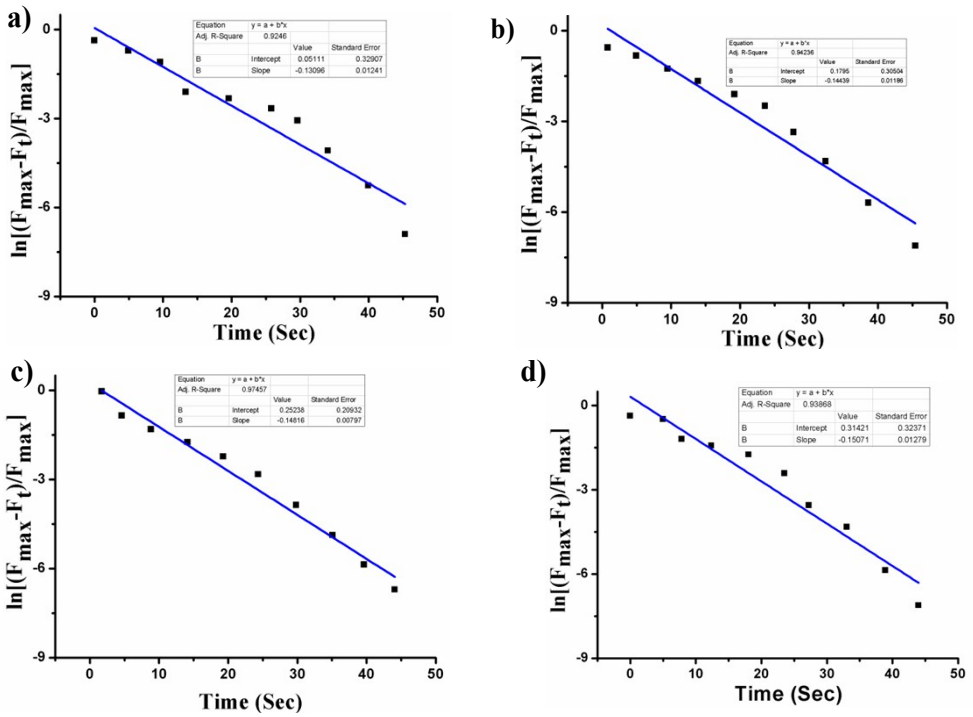

Fig. S23 (a) Pseudo first-order kinetic plot of reaction of **HNBM** (0.2 μM) with various concentration of DCP a) 40 μM b) 80 μM c)100 μM d) 150 μM in acetonitrile. Thus the Pseudo first-order rate constant of the reaction at 25^{o}C, K= -0.15071 Sec-1.

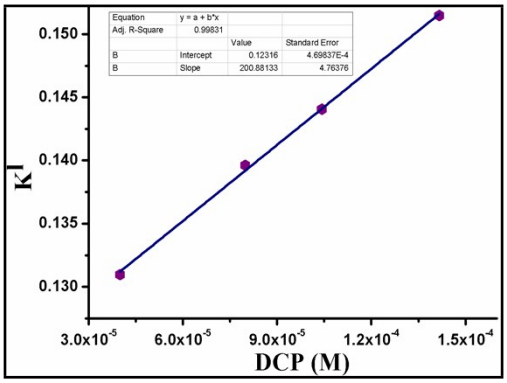

Fig. S24 Plot of the observed **k/** versus the concentration of DCP for the pseudo first-order reaction of **HNBM** (2 µM) with varying concentration of DCP (0-150 µM). **Slope = 200.88 $M^{-1}Sec^{-1}$.**

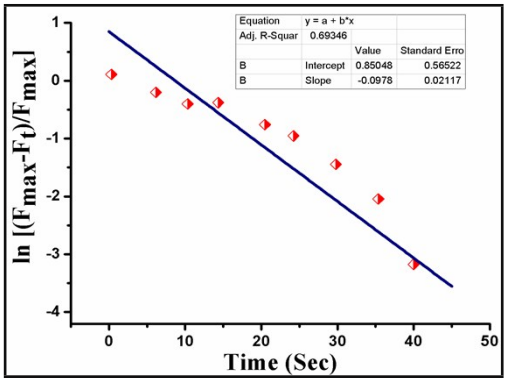

Fig. S25 Pseudo first-order kinetic plot of reaction of **HBBM** (2 µM) with DCP (40 µM). Rate constant of the reaction at 25°C, K= -0.097 Sec-1

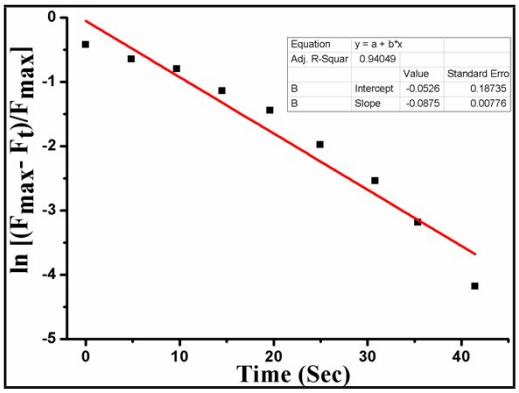

Fig. S26 Pseudo first-order kinetic plot of reaction of **HMBM** (2 µM) with DCP (40 µM). Rate constant of the reaction at 25°C, K=- 0.087 Sec-1.

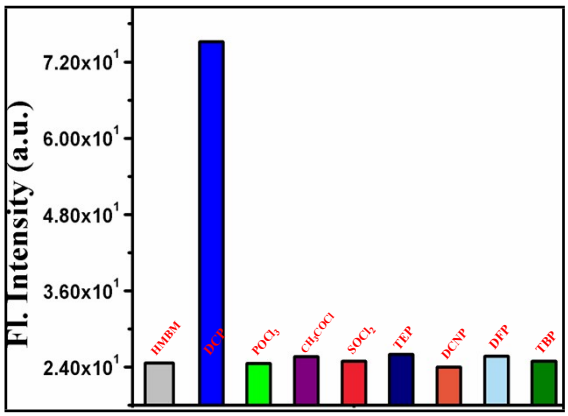

Fig. S27 Fluorescence intensity response of **HMBM** (2 μM) to DCP (40 μM) and other interferents (100 μM). The emission intensity was measured at λem = 483 nm.

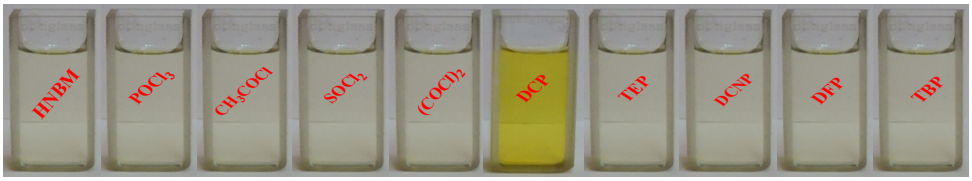

Fig. S28 The visible color changes of **HNBM** in aq. CH_3CN (CH_3CN: H_2O = 7:3 v/v, 10 mM HEPES buffer, pH = 7.4) upon addition of various interferents.

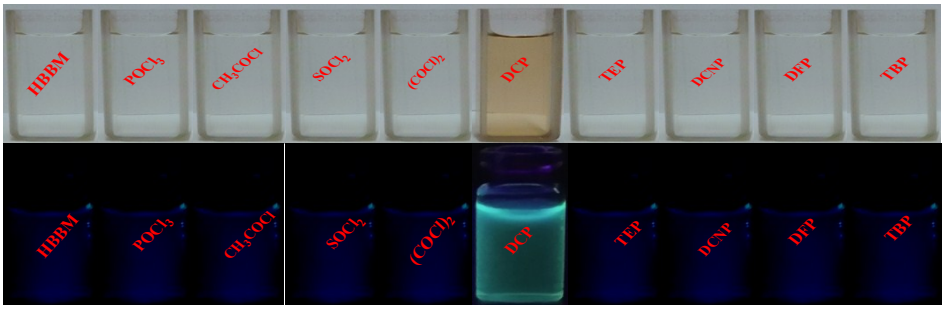

Fig. S29 The visible color (top) and fluorescence (bottom) changes of **HBBM** in aq. CH_3CN (CH_3CN: H_2O = 7:3 v/v, 10 mM HEPES buffer, pH = 7.4) upon addition of various interferents.

Fig. S30 Fluorescence changes of **HMBM** in aq. CH_3CN (CH_3CN: H_2O = 7:3 v/v, 10 mM HEPES buffer, pH = 7.4) upon addition of various interferents.

Computational details:

Geometries have been optimized using the B3LYP/6-31G (d, p) level of theory The geometries are verified as proper minima by frequency calculations. Time-dependent density functional theory calculation has also been performed at the same level of theory. All calculations have been carried out using Gaussian 09 program. The numbers in parentheses are the excitation energy in wavelength. [b] Oscillator strength. [c] H stands for HOMO and L stands for LUMO.

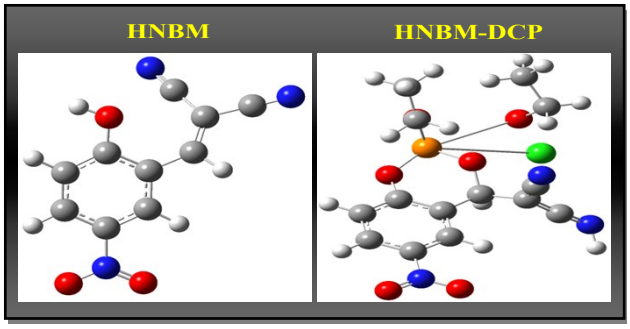

Fig. S31 Energy Optimized structures of **HNBM and HNBM-DCP**

Table S1: Selected electronic excitation energies (eV), oscillator strengths (f) and main configurations of **HNBM** and **HNBM-DCP**. The data were calculated by TDDFT//B3LYP/6-311+G (*d,p*) based on the optimized ground state geometries.[a] Only selected excited states were considered. The numbers in parentheses are the excitation energy in wavelength. [b] Oscillator strength. [c] H stands for HOMO and L stands for LUMO.

Molecules	Electronic Transition	Excitation Energy[a]	f[b]	Composition[c]	(composition) %
HNBM	$S_0 \rightarrow S_1$	3.1886 eV 346.09 nm	0.1275	H → L+1	74.8
	$S_0 \rightarrow S_6$	4.2434 eV 311.16 nm	0.2891	H -1→ L	68.6
HNBM-DCP	$S_0 \rightarrow S_1$	3.9418 eV 396.98 nm	0.2140	H → L	64.3
	$S_0 \rightarrow S_2$	4.2187 eV 369.86 nm	0.2504	H-1 → L	66.2

Table S2: Energies of the highest occupied molecular orbital (HOMO) and lowest unoccupied molecular orbital (LUMO) of **HNBM** and **HNBM - DCP.**

Species	E_{HOMO} (a.u)	E_{LUMO}(a.u)	ΔE(a.u)	ΔE(eV)	ΔE(kcal/mol)
HNBM	-0.27131	-0.1147	0.1565	4.2593	98.2037
HNBM-DCP	-0.29688	-0.18415	0.11273	3.06749	70.7380

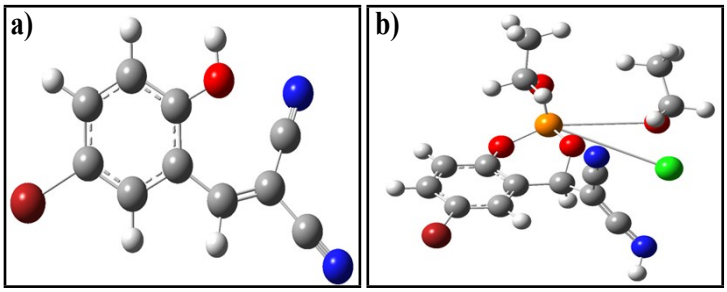

Fig. S32 Energy Optimized structures of **HBBM and HBBM-DCP**

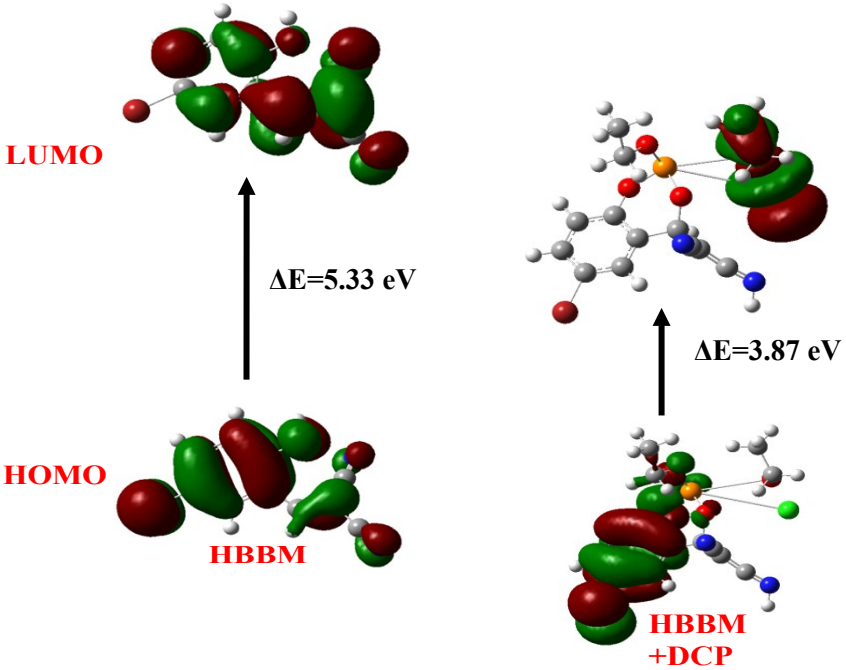

Fig. S33 Energy difference in the respective HOMO and LUMO of **HBBM** and **HBBM-DCP**.

Table S3: Selected electronic excitation energies (eV), oscillator strengths (f) and main configurations of **HBBM** and **HBBM-DCP.** The data were calculated by TDDFT//B3LYP/6-311+G (d,p) based on the optimized ground state geometries. [a] Only selected excited states were considered. The numbers in parentheses are the excitation energy in wavelength. [b] Oscillator strength. [c] H stands for HOMO and L stands for LUMO.

Molecules	Electronic Transition	Excitation Energy[a]	f[b]	Composition[c]	(composition) %
HBBM	$S_0 \rightarrow S_1$	3.1702 eV 349.09 nm	0.2075	H → L	93.8
	$S_0 \rightarrow S_9$	4.0234 eV 307.16 nm	0.5191	H -1→ L	93.6
HBBM-DCP	$S_0 \rightarrow S_1$	3.9018 eV 389.98 nm	0.2140	H → L	56.3
	$S_0 \rightarrow S_2$	4.8187 eV 369.86 nm	0.2504	H-1 → L	51.2

Table S4: Energies of the highest occupied molecular orbital (HOMO) and lowest unoccupied molecular orbital (LUMO) of **HBBM** and **HBBM - DCP.**

Species	**E_{HOMO} (a.u)**	**E_{LUMO}(a.u)**	**ΔE(a.u)**	**ΔE(eV)**	**ΔE(kcal/mol)**
HBBM	-0.23596	-0.03986	0.1961	5.3360	122.05275
HBBM-DCP	-0.24668	-0.10415	0.1425	3.8783	89.36631

Quantum yield calculation:

Here, the quantum yield ϕ was measured by using the following equation:

$\phi_x = \phi_s (F_x / F_s)(A_s / A_x)(n_x^2/ n_s^2)$

Where,

X & S indicate the unknown and standard solution respectively, ϕ = quantum yield,

F = area under the emission curve, A = absorbance at the excitation wave length,

n = index of refraction of the solvent. Here ϕ measurements were performed using Fluorescein in 0.1 M NaOH as standard (ϕ = 0.79) and anthracene in ethanol as standard (0.27) were used .For standard (s) Fluorescein in 0.1 M NaOH and anthracene in ethanol the following values were determined:

n_s = 1.3330 (for 0.1 M NaOH); n_x=1.344 (for CH_3CN); ϕ = 0.79.

n_s = 1.5948 (ethanol); n_x=1.344 (for CH_3CN); ϕ = 0.27.

Using the above equation, we calculated quantum yield of probes.

Probes	**Quantum yield** (ϕ)
HNBM	0.03
HNBM-DCP at 503 nm	0.17
HBBM	0.008
HBBM-DCP at 529 nm	0.02
HMBM	0.025
HNBM-DCP at 483 nm	0.135

Table S5: Quantum yield data

MTT assay:

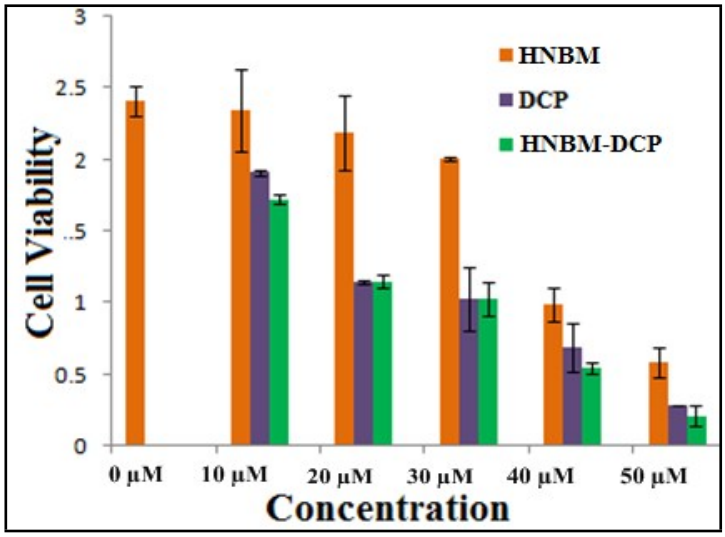

Fig.S34 Cell viability assay of **Hep-2** cells to observe the cytotoxic effect of **HNBM** and DCP**.**

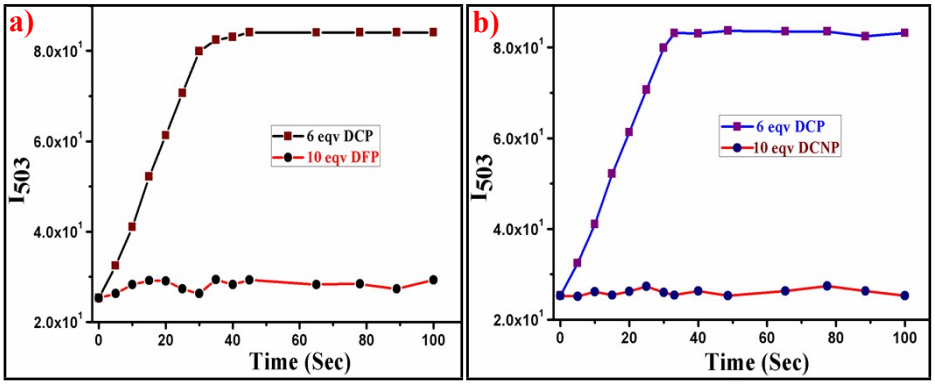

Fig. S35 a) Time-dependent fluorescence intensity of **HNBM** (2 μM) at 503 nm with 6 equiv addition of DCP (40 μM) and 10 equiv addition of DFP, excitation at 373 nm. b) Time-dependent fluorescence intensity of **HNBM** (2 μM) at 503 nm with 6 equiv addition of DCP (40 μM) and 10 equiv addition of DCNP, excitation at 373 nm.

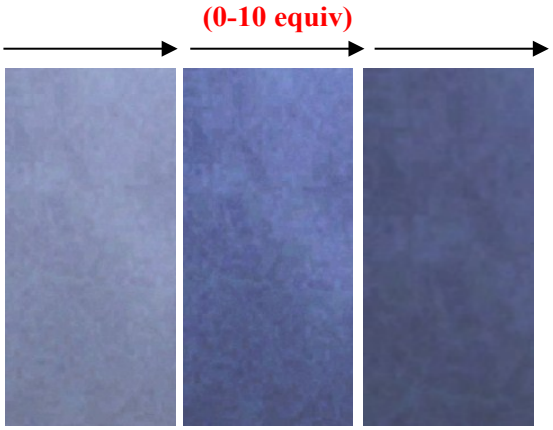

Fig. S36 Fluorescence photos of **HNBM** soaked cellulose test papers have been exposed to various concentration (0- 10 equiv) of HCl for 1 min.

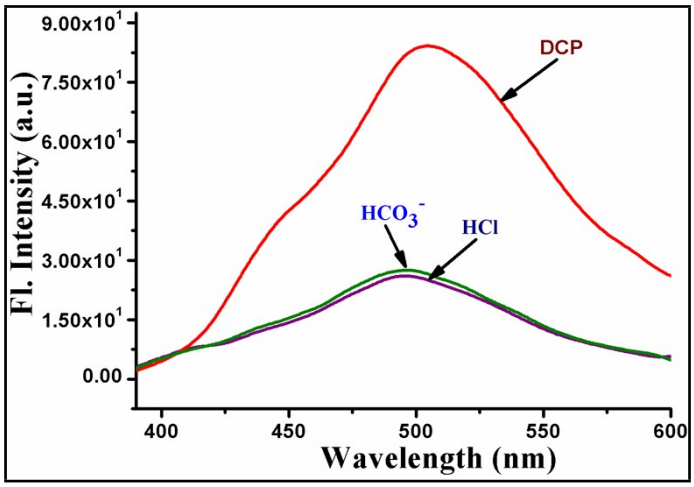

Fig. S37 Comparative fluorescence spectra of **HNBM** (2 μM) in acetonitrile-water (10 mM HEPES buffer, 7:3 V/V, pH 7.4, at 25°C) upon addition of DCP (40 μM), HCO_3^- (100 μM) and HCl (100 μM), λ_{exc} =373 nm.

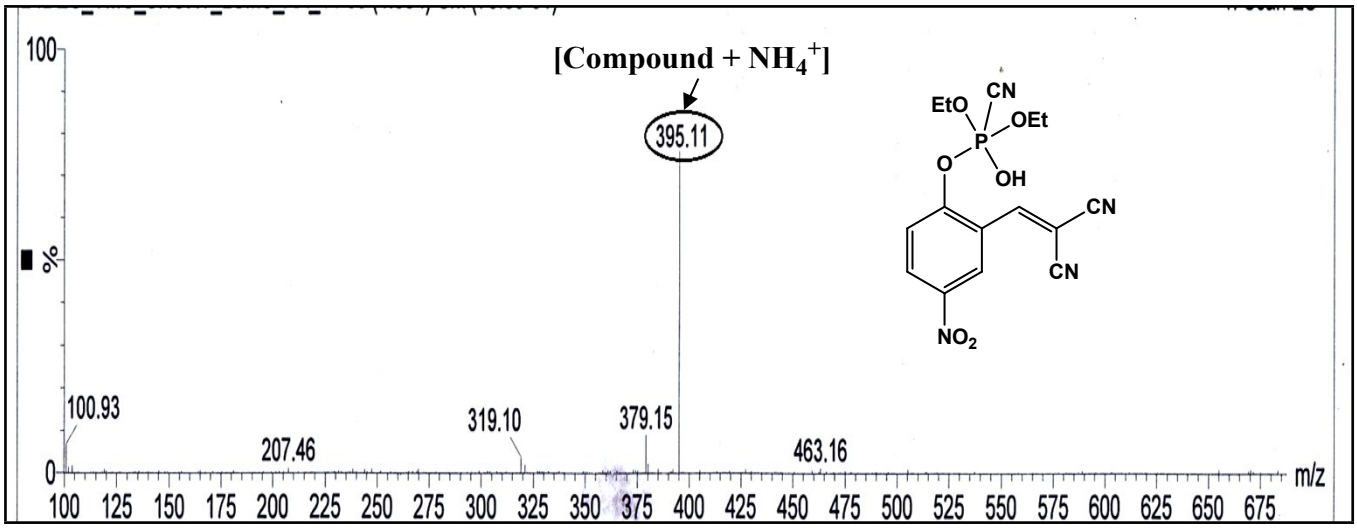

Fig. S38 LCMS of **HNBM-DCNP**.

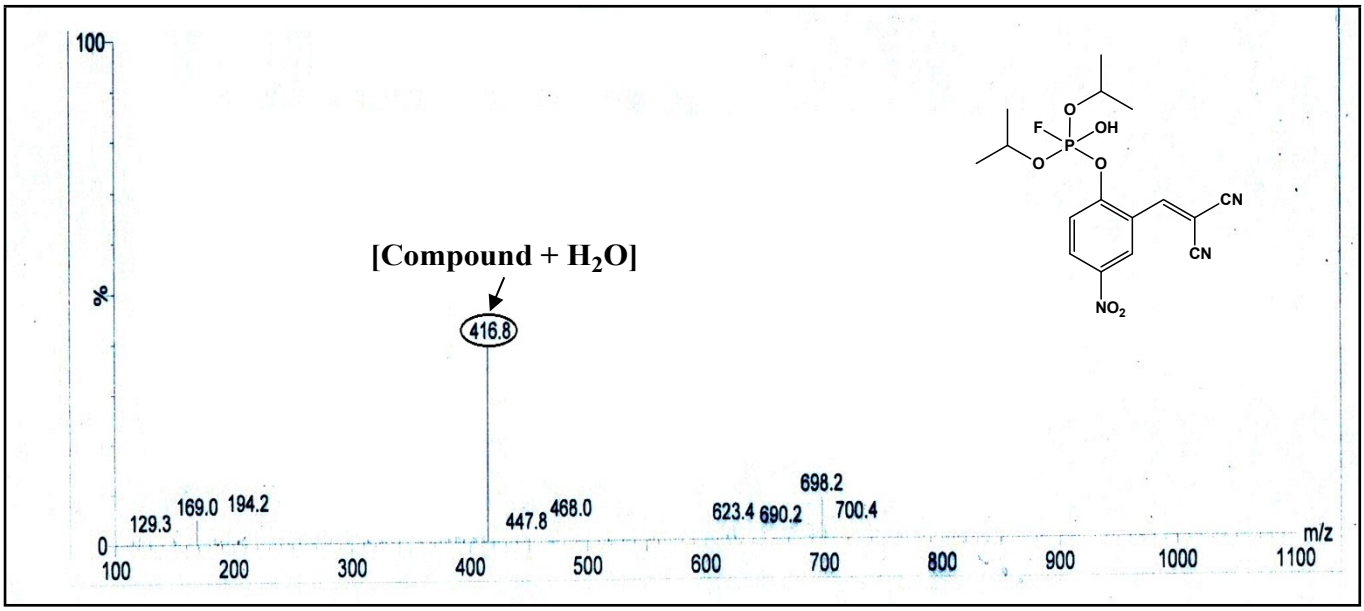

Fig. S39 LCMS of **HNBM-DFP**.